

MODEL-FITTING AND MODEL-FREE ANALYSIS OF THERMAL DECOMPOSITION OF PALLADIUM ACETYLACETONATE [Pd(acac)₂]

B. Janković* and S. Mentus

Faculty of Physical Chemistry, University of Belgrade, Studentski trg 12-16, P.O. Box 137, 11001 Belgrade, Serbia and Montenegro

The non-isothermal decomposition process of the powder sample of palladium acetylacetone [Pd(acac)₂] was investigated by thermogravimetric (TG) and the X-ray diffraction (XRD) techniques. Model-free isoconversional method of Tang, applied to the investigated decomposition process, yield practically constant apparent activation energy in the range of $0.05 \leq \alpha \leq 0.95$. It was established, that the Coats–Redfern (CR) method gives several statistically equivalent reaction models, but only for the phase-boundary reaction models (R2 and R3), the calculated value of the apparent activation energy (E) is nearest to the values of E obtained by the Tang's and Kissinger's methods.

The apparent activation energy value obtained by the IKP method ($132.4 \text{ kJ mol}^{-1}$) displays a good agreement with the value of E obtained using the model-free analysis ($130.3 \text{ kJ mol}^{-1}$). The artificial isokinetic relationship (aIKR) was used for the numerical reconstruction of the experimental integral model function, $g(\alpha)$. It was established that the numerically reconstructed experimental function follows R3 reaction model in the range of α , taken from model-free analysis. Generally, decomposition process of Pd(acac)₂ starts with initial nucleation which was characterized by rapid onset of an acceleratory reaction without presence of induction period.

Keywords: decomposition, model-fitting, model-free, non-isothermal kinetics, palladium acetylacetone

Introduction

Organometallic complexes have gained widespread use in catalysis over the past few decades. In particular, precious metal complexes have been used extensively as catalysts in many synthetic organic reactions [1–8] including industrial-scale reactions. Metal catalysts often contain organic ligands, and standard analyses of metals by ion selective electrodes (ISEs) and other electrochemical techniques are, however, for metal ions free of organic ligands [9–11]. The organic ligands usually need to be decomposed or removed to free the metals prior to their qualitative and quantitative analysis.

Poston and Reisman [12] are investigating the relative stabilities of palladium acetylacetone and palladium hexafluoroacetylacetone using DTA and mass loss analysis. In general, the acetylacetones decompose in the solid-state at relatively low temperatures ($100\text{--}200^\circ\text{C}$), with several of them exhibiting appreciable vapor pressures at temperatures below which their decomposition rate is significant. At the heating rates employed, $\leq 2^\circ\text{C min}^{-1}$, palladium acetylacetone tends to decompose upon heating in either an inert or oxidizing atmosphere before significant quantities volatilize. Heating palladium acetylacetone in argon, at $\leq 2^\circ\text{C min}^{-1}$, shows the onset of

an endotherm at approximately 196°C , at the conclusion of which a product containing 75% palladium was found, the remainder comprised of carbon, hydrogen and oxygen [12]. They were found, that in oxidizing atmosphere at the same heating rate, Pd(acac)₂ decomposes exothermically at 180°C yielding essentially pure palladium. Continued heating in oxygen, to 800°C results in pure PdO. At 900°C , the PdO decomposes yielding pure palladium.

Our principal objective is the kinetic analysis of non-isothermal decomposition of palladium acetylacetone (Pd(acac)₂) (determination of full kinetic triplet: pre-exponential factor (A), apparent activation energy (E) and analytical form of reaction model function ($f(\alpha)$) by applying model-fitting and model-free approaches [13]. In the modern literature, there is no information about the non-isothermal decomposition of palladium acetylacetone from the point of view of solid-state kinetics.

Experimental

Materials and methods

Palladium acetylacetone was synthesized by precipitation from the solution of PdCl₂ and acetylacetone in ethanol. The precipitate was washed by ethanol and

* Author for correspondence: bojanjan@ffh.bg.ac.yu

dried under vacuum of approximately 10 mbar at room temperature.

Thermal decomposition of acetylacetone samples was studied by thermogravimetric technique using a TA SDT 2960 thermobalance. The average mass of samples was about 4 mg. Purging gas was a nitrogen (99.9995 vol%) at a flowing rate of 90 mL min⁻¹. The flow of pure filtered nitrogen carrier gas was supplied from a high-pressure (HP) cylinder. The furnace temperature rose linearly at the following heating rates (β): $\beta=2, 5, 10, 15$ and $30^{\circ}\text{C min}^{-1}$, in the temperature range from an ambient one up to 350°C . The microphotograph of the samples upon decomposition was taken by scanning electron microscope of type JEOL JSM-6460. The X-ray powder diffraction (XRPD) patterns were collected using a Philips PW-1050 automatic diffractometer with a CuK _{$\alpha_{1,2}$} line of 1.5418 nm.

Kinetic analysis

Kinetics of solid-state reactions is usually described by the following equation:

$$\frac{d\alpha}{dt} = A \exp\left(-\frac{E}{RT}\right) f(\alpha) \quad (1)$$

where α is the extent of conversion defined as $\alpha = (m_0 - m_t)/(m_0 - m_f)$ (m_t represents the mass of the sample at arbitrary time t (or temperature T), whereas m_0 and m_f are the mass of the sample at the beginning and at the end of the process, respectively), A is the pre-exponential factor, E is the apparent activation energy, R is the gas constant and $f(\alpha)$ is the reaction model function. Moreover, taking into account that under non-isothermal condition the heating rate is $\beta=dT/dt$, then from Eq. (1) we have Eq. (2):

$$\frac{d\alpha}{dT} = \frac{d\alpha}{dt} \frac{dt}{dT} = \left(\frac{A}{\beta} \right) \exp\left(-\frac{E}{RT}\right) f(\alpha) \quad (2)$$

Most of the methods that describe the kinetics of reactions in solids use Eq. (2) as well as several approximation of its integral form:

$$g(\alpha) = \frac{A}{\beta} \int_0^T \exp\left(-\frac{E}{RT}\right) dT = \left(\frac{AE}{\beta R} \right) \int_x^{\infty} \frac{\exp(-x)}{x^2} dx = \left(\frac{AE}{\beta R} \right) p(x) \quad (3)$$

where $g(\alpha)$ is the integral form of the model function and $p(x)$ represents the ‘temperature integral’, which can not be analytically integrated, where $x=E/RT$. To overcome this difficulty, the ‘temperature integral’ has been solved using approximation methods, series expansions, and numerical solution methods [14].

Model-free methods

However, due to the complexity of the kinetic description concerning the solid-state decomposition processes it is usually assumed that the apparent activation energy is not a constant value but depends on α [15, 16]. Therefore, in order to establish if such dependence exists or not, the kinetic procedure adopted in this work was first based on two multi-heating rate methods. Both approaches determine the apparent activation energy using thermal analysis data carried out at different fixed heating rates without choosing a priori a defined model function. In particular, the first kinetic method used was the isoconversional method of Tang *et al.* [17], that is based on Eq. (3), with approximate formula of high accuracy for Arrhenius temperature integral [17] in linear form:

$$\ln \frac{\beta}{T^{1.894661}} = \ln \frac{AE}{Rg(\alpha)} + 3.635041 - 1.894661 \ln E - 1.001450 \frac{E}{RT} \quad (4)$$

At any selected value of α , from the slope of the related regression straight line derived by the $\ln(\beta/T^{1.894661})$ vs. $1/T$ plot, the corresponding E value is derived as a function of α . The present kinetic study was also performed using the Kissinger method [18, 19] that uses the following equation:

$$\ln \left(\frac{\beta}{T_p^2} \right) = \ln \left(\frac{AR}{E} \right) + \left(-\frac{E}{R} \right) \frac{1}{T_p} \quad (5)$$

where T_p is the DTG peak temperature at a given heating rate. From the slope of Eq. (5) a single apparent activation energy value (E) for each step of mass loss is given.

Model-fitting methods

For non-isothermal experiments, model-fitting involves fitting different models to $\alpha-T$ curves and simultaneously determining E and A [20]. Subsequently, TG data derived by a single linear heating rate experiment were fitted to some of the integral model functions $g(\alpha)$ reported in the literatures [20–22] using the Coats–Redfern (CR) method [23]. This method makes the assumption that the integral model function

$$\ln \left[\frac{g_j(\alpha)}{T^2} \right] = \ln \left(\frac{A_j R}{\beta E} \right) - \frac{E_j}{RT} \quad (6)$$

where the subscript j is related to the selected reaction model. From the slope of the linear regression obtained by plotting $\ln[g_j(\alpha)/T^2]$ vs. $1/T$, the corresponding kinetic parameters E_j and A_j are obtained for each

model function j . These kinetic parameters related to all the different model function j of the same process are linearly correlated (compensation effect).

It has been observed that the same experimental curve $\alpha=\alpha(T)$ can be described by the different model function ($f(\alpha)$). Further, the values of the apparent activation energy obtained for various $f(\alpha)$ for the single non-isothermal curve are correlated through the compensation effect [24, 25]. These observations form the basis of the IKP –invariant kinetic parameter method. In order to apply this method, $\alpha=\alpha(T)$ curves are obtained at the different heating rates (β_v , $v=1, 2, 3, \dots$) using TG technique. For each heating rate, the pairs (A_{vi}, E_{vi}) (where i corresponds to a particular extent of conversion), are determined using the CR equation (Eq. (6)). For constant value of β , a plot of $\ln[g(\alpha)/T^2]$ vs. $1/T$ is a straight line whose slope allows the evaluation of the apparent activation energy E_v and intercept, the pre-exponential factor A_v , for different reaction models $g(\alpha)$. The same procedure is repeated to obtain the pairs (E_v, A_v) for different heating rates. In addition, the calculation of the invariant activation parameters is done using the compensation relation [25–27]

$$\ln A_v = \alpha^* + \beta^* E_v \quad (7)$$

The above Eq. (7) represents a linear relationship between $\ln A$ and E and any increase in the magnitude of one parameter is offset, or compensated, by the appropriate increase of the other. Plotting $\ln A_v$ vs. E_v for the different heating rates, the compensation effect parameters α^* and β^* are obtained. These parameters follow an equation

$$\alpha^* = \ln A - \beta^* E \quad (8)$$

The plot of α^* and β^* gives the true values of kinetic parameters (A, E).

Numerical reconstruction of the experimental model function

The integrated model function $g(\alpha)$ can be numerically reconstructed using an artificial isokinetic relationship (aiKIR) [28] if E_α were practically independent of α . Once the values of $\ln A_\alpha$ and E_α are determined the integrated model function $g(\alpha)$ is reconstructed by substituting the selected estimates of A_α and E_α in Eq. (3). The explicit form of the model function can be determined by comparing the selected numerical dependence of $g(\alpha)$ vs. α with corresponding model dependencies.

Results and discussion

TG and DTG curves of the decomposition process of palladium acetylacetone ([Pd(acac)₂]) samples obtained at the different heating rates ($\beta=2, 5, 10, 20$ and $30^\circ\text{C min}^{-1}$) are shown in Figs 1 and 2.

The observed TG curves show an asymmetric character and were moved to a higher values of experimental temperature with increase in heating rate (Fig. 1). The total mass loss for considered process at all heating rates was found to be 71.47%. The observed DTG curves manifested the similar behaviour as TG curves, where the peak temperature (T_p) values increasing with increase in heating rate, β (Table 1).

Figure 3 shows the rate–temperature ($d\alpha/dt-T$) curves for decomposition process of palladium acetylacetone at the different heating rates.

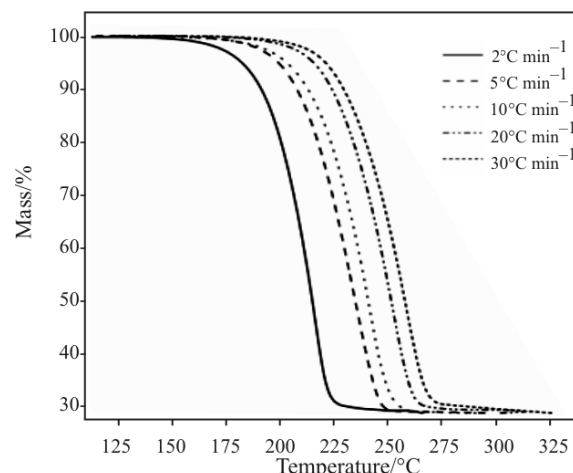


Fig. 1 TG curves for the non-isothermal decomposition process of palladium acetylacetone samples in nitrogen atmosphere

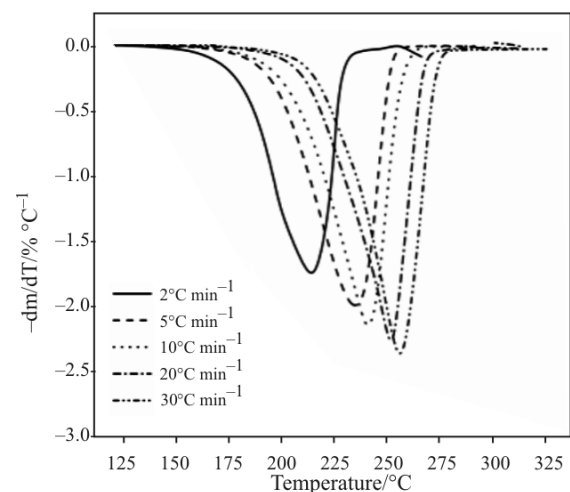


Fig. 2 DTG curves for the non-isothermal decomposition process of palladium acetylacetone samples in nitrogen atmosphere

Table 1 Values of T_p and α_p for the non-isothermal decomposition process of palladium acetylacetonate ($\text{Pd}(\text{acac})_2$), determined by thermogravimetric analysis at the different heating rates

$\beta/\text{°C min}^{-1}$	$T_p/\text{°C}$	α_p
2	215	0.73
5	235	0.73
10	240	0.69
20	250	0.70
30	255	0.72

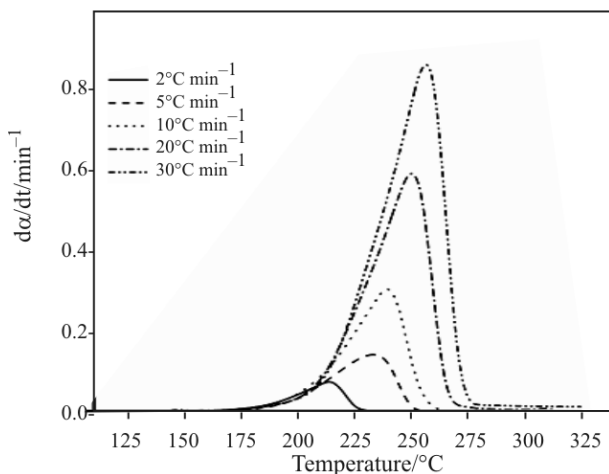


Fig. 3 Experimental reaction rate curves (da/dt vs. T) for the decomposition process of palladium acetylacetonate under the nitrogen atmosphere at the different heating rates

As can be seen from Fig. 3, the maximal rate of the investigated process increases with increase in heating rate. The maximums of the rate–temperature curves were moved to a range of higher values of temperature (Fig. 3) and this behaviour coincides with behaviour of DTG curves (Fig. 2). The both, DTG and rate–temperature curves exhibited the one clearly peak at all heating rates. From these results, we may concluded, that the investigated decomposition process can follow the single-step reaction mechanism. However, this observation is some roughly, and because of that, the further analysis is necessary.

Figure 4 shows the dependence of da/dt vs. α for the investigated decomposition process of palladium acetylacetonate at the considered heating rates.

It can be seen from Fig. 4, that the values of α which corresponds to the maximum values of rate of process (α_p) falls in the range of $0.69 \leq \alpha_p \leq 0.73$ (Table 1). From the Dollimore's procedure for the identification of reaction mechanism [29–31], which is based on the theoretical positions of α_p values in α scale for the various types of solid-state mechanisms, we can conclude that the investigated decomposition process belongs to the group of phase-boundary con-

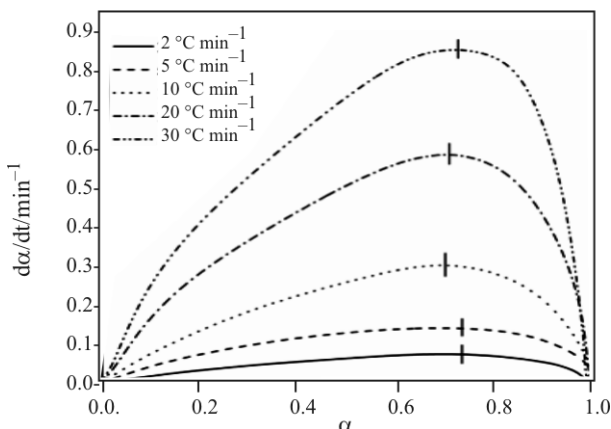


Fig. 4 The dependence of da/dt vs. α for the decomposition process of palladium acetylacetonate at the different heating rates. Short solid lines represents the maximums of the curves which corresponds to α_p values

trolled reactions (mechanisms: R2 ($0.73 \leq \alpha_p \leq 0.74$) or R3 ($\alpha_p = 0.69$)). It can be pointed out, that this approach is useful for the basic classification of possible kinetic model, but it is not sufficient for an unambiguous determination of true reaction model. The non-isothermal decomposition process of palladium acetylacetonate was analyzed by Tang (T) isoconversional method. For all sets of α values, the linear isoconversional plots result in a linear correlation coefficients larger than 0.99. The dependences of E and $\ln[A/g(\alpha)]$ values on α are displayed in Fig. 5.

As shown in Fig. 5, the value of apparent activation energy hardly varies with the extent of conversion (α). Practically constant E values around $130.3 \pm 1.9 \text{ kJ mol}^{-1}$ were found (changes lie within the associated uncertainties). Alternatively, $\ln[A/g(\alpha)]$ – α plot demonstrates an identical manner (Fig. 5), which it may suggest that both the apparent activation energy (E) and the pre-exponential factor (A) are practi-

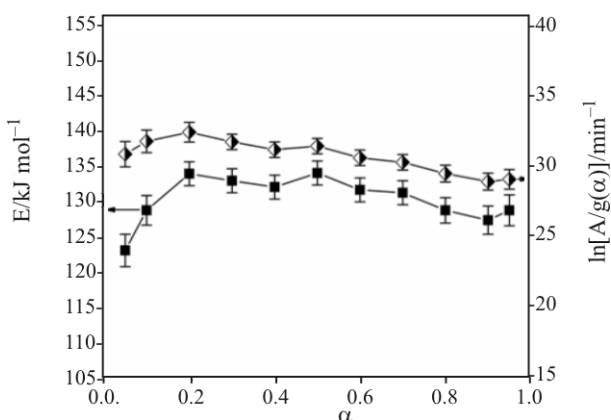


Fig. 5 The dependence of the apparent activation energy (E) and $\ln[A/g(\alpha)]$ values on the extent of conversion (α) (T-method) for the non-isothermal decomposition process of palladium acetylacetonate

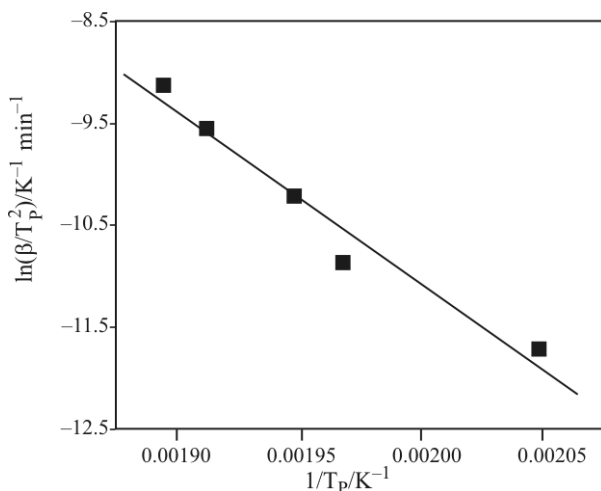


Fig. 6 Kissinger plot for the decomposition process of palladium acetylacetone

cally independent on the extent of conversion. On the other hand, from the slope of the regression line obtained by fitting the $\ln(\beta/T_p^2)$ experimental data vs. T_p^{-1} (Fig. 6) according to Eq. (4), the apparent activation energy of the investigated decomposition process equal to 138.0 ± 2.2 kJ mol⁻¹ is found. The value of pre-exponential factor (A), for the considered decomposition process is the following: $A = 7.00 \cdot 10^{13}$ min⁻¹.

The value of the apparent activation energy obtained by the Kissinger's method is higher than value of E obtained by the Tang (T) method (130.3 kJ mol⁻¹). It can be pointed out, that the difference between E values calculated from the above mentioned methods does not large ($\Delta E < 10$ kJ mol⁻¹), which represent a satisfactory result. The kinetic parameters for the decomposition process of Pd(acac)₂ are also determined by CR method for all model functions used in this work, and given in Tables 2 and 3 with their linear correlation coefficient (r) values [32]. The validity of reaction model functions was tested by a statistical F-test [33, 34].

A single function can not be discriminated since the five phase-boundary (R2; R3) and two- and three-dimensional diffusion models (D2; D3; D4) seem to be statistically equivalent fitting models. It can be observed, that only for R2 and R3 models, the calculated value of the apparent activation energy is nearest to the values of E obtained by the Tang's and Kissinger's methods, separately at the 10°C min⁻¹.

In order to apply the IKP method, the conversion range in which the value of E is practically constant has to be determined and that has been done through the above methods. For determining the compensation effect parameters (α^* , β^*), CR method has been

Table 2 Arrhenius parameters related to the decomposition process of Pd(acac)₂ at 2 and 5°C min⁻¹ obtained by the Coats–Redfern method for the most commonly used model functions

Model	$\beta=2^\circ\text{C min}^{-1}$				$\beta=5^\circ\text{C min}^{-1}$			
	$\ln A$	$E/\text{kJ mol}^{-1}$	r	F-test ^b	$\ln A$	$E/\text{kJ mol}^{-1}$	r	F-test ^b
P1	2.42	25.1	-0.9976	1476.386	2.21	22.2	-0.9839	273.597
P2	5.46	36.0	-0.9980	1761.532	4.95	32.3	-0.9867	331.070
P3	11.29	58.0	-0.9983	2080.180	10.18	52.6	-0.9888	394.967
P4	44.61	189.6	-0.9986	2561.149	39.80	174.1	-0.9909	490.605
R1	28.11	123.8	-0.9986	2434.622	25.16	113.3	-0.9905	465.546
R2	32.28	141.8	-0.9997 ^a	10799.658	29.54	132.8	-0.9988	3606.960
R3	33.74	148.7	-0.9986	2571.612	31.18	140.7	-0.9997 ^a	13022.744
F1	38.97	164.2	-0.9941	585.256	36.99	158.9	-0.9972	1580.618
F3/2	46.20	191.3	-0.9811	180.387	45.67	192.6	-0.9816	237.961
F2	54.56	222.7	-0.9632	89.829	56.02	233.0	-0.9570	97.911
F3	73.81	295.4	-0.9255	41.793	79.82	326.5	-0.9100	43.338
A3/2	24.31	106.8	-0.9938	560.144	23.25	103.2	-0.9970	1510.327
A2	16.88	78.2	-0.9935	535.469	16.28	75.3	-0.9969	1441.140
A3	9.30	49.5	-0.9929	487.457	9.17	47.5	-0.9966	1306.208
A4	5.40	35.1	-0.9922	441.282	5.49	33.6	-0.9962	1176.099
D1	60.97	255.4	-0.9987	2626.037	54.31	234.9	-0.9912	503.427
D2	66.06	277.1	-0.9999 ^a	52341.542	59.48	257.6	-0.9965	1262.179
D3	72.03	305.3	-0.9987	2680.983	66.13	289.5	-0.9997 ^a	14063.192
D4	67.00	286.4	-0.9999 ^a	30618.464	60.61	267.9	-0.9981	2426.415

^aStatistically equivalent models, ^bStatistical F-distribution function [33, 34]

Table 3 Arrhenius parameters related to the decomposition process of Pd(acac)₂ at 10, 20 and 30°C min⁻¹ obtained by the Coats–Redfern method for the most commonly used model functions

Model	$\beta=10^\circ\text{C min}^{-1}$				$\beta=20^\circ\text{C min}^{-1}$				$\beta=30^\circ\text{C min}^{-1}$			
	lnA	E/kJ mol ⁻¹	r	F-test ^b	lnA	E/kJ mol ⁻¹	r	F-test ^b	lnA	E/kJ mol ⁻¹	r	F-test ^b
P1	2.72	21.8	-0.9910	493.118	4.00	24.5	-0.9875	353.752	4.09	23.6	-0.9870	302.701
P2	5.42	31.9	-0.9926	602.178	6.86	35.5	-0.9895	423.504	6.87	34.4	-0.9892	364.946
P3	10.55	52.0	-0.9939	724.532	12.32	57.4	-0.9911	500.714	12.17	55.9	-0.9909	433.993
P4	39.59	172.4	-0.9951	909.563	43.40	189.1	-0.9928	615.794	42.26	184.7	-0.9926	537.088
R1	25.24	112.2	-0.9948	860.877	28.03	123.3	-0.9924	585.688	27.38	120.3	-0.9923	510.101
R2	29.28	130.5	-0.9997 ^a	16123.178	32.07	142.0	-0.9989 ^a	4090.199	31.55	139.8	-0.9985	2721.976
R3	30.72	137.7	-0.9998 ^a	30944.615	33.52	149.4	-0.9996 ^a	11284.242	33.01	147.3	-0.9993 ^a	5526.519
F1	35.97	153.9	-0.9973	1640.946	38.77	165.9	-0.9981	2302.850	38.21	163.9	-0.9984	2461.911
F3/2	43.35	182.8	-0.9862	319.220	46.15	195.5	-0.9879	365.018	45.35	192.9	-0.9912	446.769
F2	51.99	216.8	-0.9692	139.187	54.77	230.2	-0.9708	147.324	53.57	226.5	-0.9788	182.300
F3	71.91	295.6	-0.9334	60.913	74.65	310.6	-0.9352	60.712	72.53	304.3	-0.9501	74.158
A3/2	22.79	99.8	-0.9971	1568.239	24.89	107.8	-0.9980	2203.413	24.64	106.4	-0.9983	2348.599
A2	16.09	72.8	-0.9970	1496.514	17.86	78.8	-0.9979	2105.380	17.76	77.7	-0.9982	2237.208
A3	9.25	45.8	-0.9967	1356.172	10.68	49.7	-0.9977	1913.735	10.73	48.9	-0.9980	2020.424
A4	5.71	32.3	-0.9963	1220.258	6.97	35.2	-0.9974	1728.344	7.10	34.6	-0.9978	1812.027
D1	53.82	232.6	-0.9952	934.529	58.64	255.0	-0.9930	631.189	57.00	249.1	-0.9928	550.891
D2	58.68	254.5	-0.9986	3147.878	63.53	277.4	-0.9972	1603.874	62.10	272.7	-0.9970	1312.808
D3	64.57	283.6	-0.9999 ^a	31966.762	69.42	307.2	-0.9996 ^a	12124.441	68.04	303.2	-0.9993 ^a	5919.451
D4	59.59	264.0	-0.9995 ^a	8155.639	64.44	287.1	-0.9985	2937.629	63.04	282.7	-0.9982	2162.290

^aStatistically equivalent models, ^bStatistical F-distribution function [33, 34]

applied in the range of the extent of conversion where E is independent on α ($0.05 \leq \alpha \leq 0.95$). The apparent compensation effect is observed for each heating rate for the process under investigation and presented in Fig. 7.

A compensation effect of this kind is classified as artificial compensation effect which occurs on fitting the various reaction models to the same set of non-isothermal kinetic data [35]. The values of α^* and β^* were calculated from the intercepts and the slopes of the straight lines obtained in Fig. 7. The values of the apparent compensation effect parameters (α^*, β^*) obtained at the different heating rates (β) are presented in Table 4.

A linear regression from the straight-line plot of $\alpha^* = \ln A - \beta^* E$ allows computation of the kinetic parameters (A, E). From Eq. (8) one obtains: $A = 1.10 \cdot 10^{13} \text{ min}^{-1}$ and $E = 132.4 \text{ kJ mol}^{-1}$. Table 4 also shows the values of isokinetic temperatures ($T_{\text{iso}} = 1/R\beta^*$) at considered heating rates. From the established results, we can see that the value of E obtained by the IKP method ($132.4 \text{ kJ mol}^{-1}$) is very close to the value of E

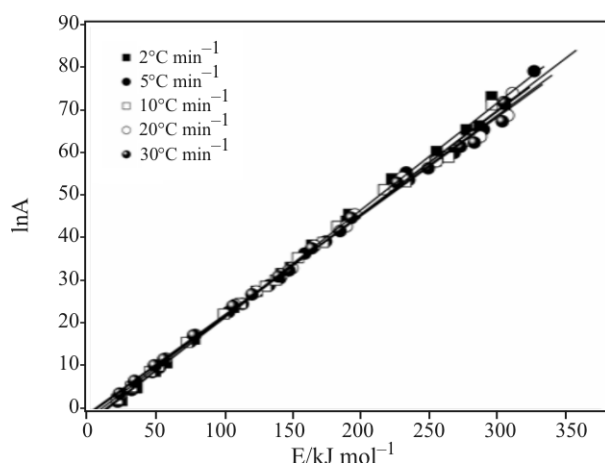


Fig. 7 Artificial compensation effect observed between the apparent activation energy and pre-exponential factor evaluated by applying the CR method, for the decomposition process of palladium acetylacetone under the nitrogen atmosphere

Table 4 Values of compensation effect parameters with corresponding values of isokinetic temperatures (T_{iso}), at five different heating rates for the non-isothermal decomposition process of palladium acetylacetone (Pd(acac)₂)

$\beta/ \text{°C min}^{-1}$	$\alpha^*/ \text{min}^{-1}$	$\beta^*/ \text{mol kJ}^{-1}$	$T_{\text{iso}}/ \text{°C}$	r
2	-3.2079	0.2523	203.5	0.9991
5	-2.6515	0.2446	218.5	0.9988
10	-1.8962	0.2411	225.7	0.9988
20	-1.1078	0.2356	237.3	0.9989
30	-0.7295	0.2328	243.5	0.9989

obtained using the model-free analysis ($130.3 \text{ kJ mol}^{-1}$). From Table 4, it can be seen that the isokinetic temperature (T_{iso}) increasing with increase in heating rate, and all T_{iso} lies in the region of the experimental temperatures. The E value from model-free analysis can be used to calculate numerically the actual model functions, $f(\alpha)$ or $g(\alpha)$. Comparison of the numerically reconstructed kinetic function with those of the theoretical models can provide a much clearer picture of the reaction mechanism and can indicate whether the mechanism changes during the course of the reaction. To reconstruct the model numerically, we must evaluate the pre-exponential factor, A . Vyazovkin and Lesnikovich [36] were the first to evaluate the pre-exponential factor by use the artificial isokinetic relationship (aiIKR). Such an analysis shows that the values of $\ln A$ are linearly related to the values of E obtained from fitting to different models. As a consequence, A for the model-free approach may be calculated as a function of the extent of conversion. Figure 8 shows the dependence of $\ln A$ values calculated from the model-free approach on the extent of conversion (α), for the non-isothermal decomposition process of palladium acetylacetone (the calculations are done for $\beta = 10 \text{ °C min}^{-1}$).

It can be observed that $\ln A$ values follow the same trend as the E values which were calculated using Tang's method (Fig. 5). With knowledge of E and A , the experimental kinetic function, $g(\alpha)$, can be calculated using Eq. (3) [36]. The numerically reconstructed experimental kinetic function, $g(\alpha)$, is shown in Fig. 9. The lines were calculated according to R2, R3, D2, D3 and D4 models. Because the kinetic function, $g(\alpha)$, depends only on α , the construction of these lines does not require knowledge of E or A . The lines are constructed from knowledge of the individual kinetic function itself.

The superposition of experimental $g(\alpha)$ function (the full circles) obtained from the model-free analysis, indicated that the kinetics of decomposition process of palladium acetylacetone could be described by a single model function. It can be easily seen from

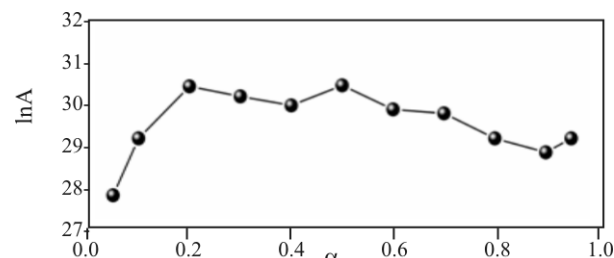


Fig. 8 The dependence of $\ln A$ values calculated from the model-free approach on the extent of conversion (α), for the non-isothermal decomposition process of palladium acetylacetone

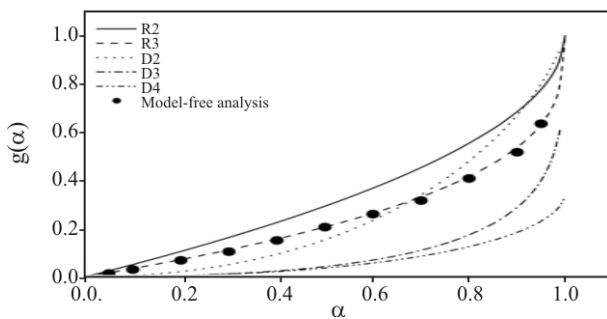


Fig. 9 Reconstruction of $g(\alpha)$ vs. α plots from model-free analysis (lines are calculated from the considered theoretical models). Key: (●) values calculated for decomposition process of $\text{Pd}(\text{acac})_2$ from the E and A values derived from model-free analysis

Fig. 9 that the kinetic process for $\text{Pd}(\text{acac})_2$ decomposition is the most probably described by R3 model with accommodated exponent $n=3$:

$$g(\alpha) = 1 - (1 - \alpha)^{\frac{1}{3}} \quad (9)$$

The contracting geometry models are based on an initial rapid (instantaneous) dense nucleation across all, or some specific, crystal faces. Close spacing of nuclei results in the rapid (low α) generation of a coherent reaction zone that advances inwards at a constant rate in the absence of diffusion effects.

On the basis of established TG curves, we can conclude that the decomposition of $\text{Pd}(\text{acac})_2$ is a single-step process, which can be presented simply by the formula:



An accompanying destruction of the ligand, if already occurs does not play significant role to the kinetics of the overall investigated process. According to the SEM microphotographs (Fig. 10), thermal decomposition commences at the outer crystal surface, yielding the ragged Pd-film, which surrounds the rest of $\text{Pd}(\text{acac})_2$ crystal.

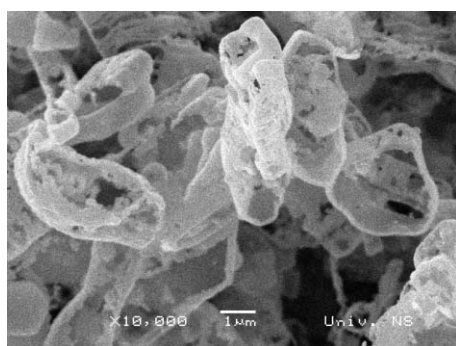


Fig. 10 SEM microphotograph of palladium (Pd) obtained by the thermal decomposition process of palladium acetylacetone $[\text{Pd}(\text{acac})_2]$

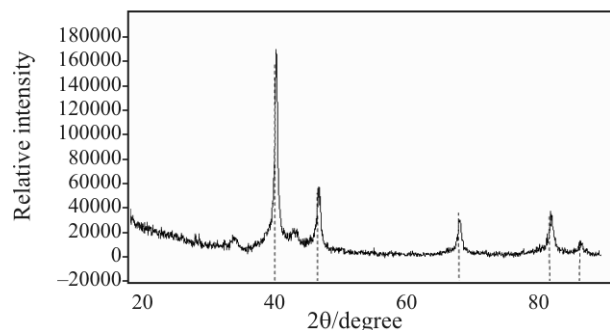


Fig. 11 X-ray diffractogram of palladium (Pd) obtained by the thermal decomposition process of $[\text{Pd}(\text{acac})_2]$. The dashed lines represent the ASTM data for palladium

The film thickens by sampling Pd atoms deliberated during the decomposition of the rest of $\text{Pd}(\text{acac})_2$, primarily at the places of close contact. It is not excluded that the film grows partly via $\text{Pd}(\text{acac})_2$ evaporation-decomposition [37–39], but however this way may not be dominant, since the mass loss caused by the sample evaporation have not been registered by TG curves. The diffractogram of the decomposition product (Fig. 11) corresponds essentially to that of Pd, with somewhat enlarged elementary cell. The width of diffraction lines indicates low degree of crystallinity. Accordingly, the mean crystal diameter calculated by means of the Scherer's formula amounts to value of 18 nm.

Generally, the decomposition process starts with initial nucleation which was characterized by rapid onset of an acceleratory reaction behavior without presence of induction period. Furthermore, the considered process was characterized by Pd particles growth in three dimensions, probably generating the spherical reaction zone.

Conclusions

The kinetics of the non-isothermal decomposition of palladium acetylacetone ($\text{Pd}(\text{acac})_2$) was accurately determined from a series of thermoanalytical experiments at the different constant heating rates. The physical characterization of decomposition product of the investigated process was analyzed by the SEM and X-ray diffraction experiments. It was established, that by applying the Tang's model-free method, the decomposition process of $\text{Pd}(\text{acac})_2$ can be described by the single step of mass loss with negligible change in the E values ($E=130.3 \pm 1.9 \text{ kJ mol}^{-1}$). It was concluded, that the Coats–Redfern (CR) method give several statistically equivalent reaction models, but only for R2 and R3 models, the calculated value of E is nearest to the values of E obtained by the Tang's and Kissinger's

methods. The use of the IKP method for the range where E is practically independent of α , led to the invariant activation parameters, which were used for the numerical evaluation of the model function, $f(\alpha)$. The apparent activation energy value (132.4 kJ mol⁻¹) obtained by the IKP method displays a very good agreement with the value of E obtained using the model-free analysis. The artificial isokinetic relationship was used for numerical reconstruction of the experimental integral model function, $g(\alpha)$. It was established that the numerically reconstructed experimental function follows the R3 reaction model in the considered range of α , taken from the model-free analysis.

Acknowledgements

The study was partially supported by the Ministry of Science and Environmental Protection of Serbia, under the following Projects 142025 and 142047 (Professor S. Mentus).

References

- 1 J. Halpern, Precious Met., 19 (1995) 411.
- 2 S. S. Stahl, Science, 309 (2005) 1824.
- 3 R. F. Heck, Palladium Reagents in Organic Synthesis, Academic Press, New York 1985.
- 4 R. Singh, M. S. Viciu, N. Kramareva, O. Navarro and S. P. Nolan, Org. Lett., 7 (2005) 1829.
- 5 J. Terao, A. Oda and N. Kambe, Org. Lett., 6 (2004) 3341.
- 6 B. M. Trost and J. Xu, J. Am. Chem. Soc., 127 (2005) 17180.
- 7 R. T. Jacobsen, Chem. Eng. Prog., 101 (2005) 20.
- 8 C. G. Anderson and S. M. Nordwick, Precious Met., 19 (1995) 123.
- 9 M. Aghamohammadi and N. Alizadeh, Anal. Chim. Acta, 480 (2003) 299.
- 10 J. Wang and K. Varughese, Anal. Chim. Acta, 199 (1987) 185.
- 11 G. Raber, K. Kalcher, C. G. Neuhold, C. Talaber and G. Kolbl, Electroanalysis, 7 (1995) 138.
- 12 S. Poston and A. Reisman, J. Electr. Mater., 18 (1989) 553.
- 13 S. Vyazovkin and C. A. Wight, Thermochim. Acta, 340–341 (1999) 53.
- 14 J. H. Flynn, Thermochim. Acta, 300 (1997) 83.
- 15 A. K. Galwey and M. E. Brown, Thermal Decomposition of Ionic Solids, Elsevier, Amsterdam 1999.
- 16 S. Vyazovkin and C. A. Wight, Annu. Rev. Phys. Chem., 48 (1997) 125.
- 17 W. J. Tang, Y. W. Liu, H. Zhang and C. X. Wang, Thermochim. Acta, 408 (2003) 39.
- 18 H. E. Kissinger, Anal. Chem., 29 (1957) 1702.
- 19 P. Budrugeac and E. Segal, J. Therm. Anal. Cal., 88 (2007) 703.
- 20 S. Vyazovkin and C. A. Wight, J. Phys. Chem. A, 101 (1997) 5653.
- 21 A. Khawam and D. R. Flanagan, J. Phys. Chem. B, 110 (2006) 17315.
- 22 A. Khawam and D.R. Flanagan, J. Pharm. Sci., 95 (2006) 472.
- 23 A. W. Coats and J. P. Redfern, Nature, 201 (1964) 68.
- 24 A. K. Galwey, Thermochim. Acta, 399 (2003) 1.
- 25 P. Budrugeac and E. Segal, Int. J. Chem. Kinet., 30 (1998) 673.
- 26 P. Budrugeac, C. Popescu and E. Segal, J. Therm. Anal. Cal., 64 (2001) 821.
- 27 P. Budrugeac, J. Therm. Anal. Cal., 89 (2007) 143.
- 28 S. Vyazovkin, Int. J. Chem. Kinet., 28 (1996) 95.
- 29 D. Dollimore, T. A. Evans, Y. F. Lee and F. W. Wilburn, Thermochim. Acta, 188 (1991) 77.
- 30 D. Dollimore, T. A. Evans, Y. F. Lee, G. P. Pee and F. W. Wilburn, Thermochim. Acta, 196 (1992) 255.
- 31 Y. F. Lee and D. Dollimore, Thermochim. Acta, 323 (1998) 75.
- 32 C. Popescu, E. Segal and C. Oprea, J. Therm. Anal. Cal., 38 (1992) 929.
- 33 N. L. Johnson and F. C. Leone, Statistics and Experimental Design in Engineering and the Physical Sciences, Wiley and Sons, New York 1977, Vol. I.
- 34 D. L. Massart, B. G. M. Vandeginste, L. M. C. Buydens, S. de Jong, P. J. Lewi and J. Smeyers-Verbeke, Handbook of Chemometrics and Qualimetrics, Part A, Elsevier, Amsterdam 1997.
- 35 S. Vyazovkin and W. Linert, Chem. Phys., 193 (1995) 109.
- 36 S. Vyazovkin and A. I. Lesnikovich, Thermochim. Acta, 128 (1988) 297.
- 37 P. P. Semyannikov, V. M. Grankin, I. K. Igumenov and A. F. Bykov, J. Phys., 4 (1995) 205.
- 38 A. G. Nasibulin, P. P. Ahonen, O. Richard, E. I. Kauppinen and I. S. Altman, J. Nanopart. Res., 3 (2001) 385.
- 39 A. G. Nasibulin, I. S. Altman and E. I. Kauppinen, Chem. Phys. Lett., 367 (2003) 771.

DOI: 10.1007/s10973-008-9118-8